London, 1974, pp 104–163.
(3) W. B. Person and D. Steele, "Molecular Spectroscopy", Vol. 2, The Chemical Society, London, 1974, pp 357, 438.
(4) J. Overend in "Infrared Spectroscopy and Molecular Structure", M. Davies, Ed., Elsevier, Amsterdam, 1963, p 345.
(5) E. B. Wilson, Jr., J. C. Decius, and P. C. Cross, "Molecular Vibrations", McGraw-Hill, New York, N.Y., 1955.
(6) K. B. Wiberg and J. J. Wendoloski, *J. Am. Chem. Soc.*, **98**, 5465 (1976).
(7) W. Meyer and P. Pulay, *J. Chem. Phys.*, **56**, 2109 (1972).
(8) G. Jalsovszky and P. Pulay, *J. Mol. Struct.*, **26**, 277 (1975).
(9) (a) D. F. Eggers, Jr., *J. Chem. Phys.*, **23**, 2211 (1955); (b) G. A. Thomas, J. A. Ladd, and W. J. Orville-Thomas, *J. Mol. Struct.*, **4**, 179 (1969); (c) R. C. Golike, I. M. Mills, W. B. Person, and B. Crawford, Jr., *J. Chem. Phys.*, **25**, 1266 (1966); (d) A. M. Thorndike, A. J. Wells, and E. B. Wilson, Jr., *ibid.*, **15**, 157 (1947); (e) H. Spedding and D. H. Whiffen, *Proc. R. Soc. London, 238*, 245 (1956).
(10) M. A. Elyashevich and M. V. Wolkenshtein, *Zh. Eksp. Teor. Fiz.*, **9**, 101 (1945).
(11) L. A. Gribov, "Intensity Theory for Infrared SPECTRA OF Polyatomic Molecules", Academy of Science Press, Moscow, 1963; Consultants Bureau, New York, N.Y., 1964.
(12) L. M. Sverdlov, M. A. Kovner, and E. P. Krainov, "Vibrational Spectra of Polyatomic Molecules", Wiley, New York, N.Y., 1974.
(13) M. V. Wolkenshtein, L. A. Gribov, M. A. Elyashevich, and Y. Y. Stepanov, "Kolebanya Molekul", Yzhdatelstvo "Nauka", Moscow, 1972.
(14) B. Galabov and W. J. Orville-Thomas, *Trans. Faraday Soc.*, **68**, 1778 (1972).
(15) J. C. Decius, *J. Mol. Spectrosc.*, **57**, 348 (1975).
(16) (a) J. F. Biarge, J. Herranz, and J. Morcillo, *An. Quim.*, **A57**, 81 (1961); (b) J. Morcillo, L. J. Zamorano, and J. M. V. Heredia, *Spectrochim. Acta*, **22**, 1966 (1969).
(17) W. T. King, G. B. Mast, and P. B. Blanchette, *J. Chem. Phys.*, **56**, 4440 (1966).
(18) W. T. King and G. B. Mast, *J. Phys. Chem.*, **80**, 2521 (1976).
(19) K. B. Wiberg and J. J. Wendoloski, *Chem. Phys. Lett.*, **45**, 180 (1977).
(20) I. M. Mills, *Spectrochim. Acta*, **19**, 1585 (1963).
(21) C. A. Coulson, "Victor Henri Memorial Volume", Desoer Liege, 1947, p 15.
(22) This can be seen from eq 21 by considering limits in which $\alpha = \pi/2$. However, localized molecular orbital values presented later also clearly confirm this statement.
(23) N. Muller and D. E. Pritchard, *J. Chem. Phys.*, **31**, 768 (1959).
(24) See ref 9a and 9c.
(25) The quantity of interest is really $\Delta\mu/\Delta S$. Using $\Delta\mu$ from eq 27, one obtains $\Delta\mu/\Delta S = [\cos(\theta - 2) - \cos(\theta + 2)]\,\mu_{CH}/\Delta S - 2[\cos(\theta - 2) + \cos(\theta + 2)]\,\delta/\Delta S$. THis last term is then identified with the rehybridization term in eq 19.
(26) G. Wipff, Ph.D. thesis, University Louis Pasteur, Strasbourg, France.
(27) K. B. Wiberg, G. M. Lampman, R. P. Ciula, D. S. Connor, P. Schertler, and J. Lavanish, *Tetrahedron*, **21**, 2749 (1965).
(28) K. B. Wiberg and D. S. Connor, *J. Am. Chem. Soc.*, **88**, 4437 (1966).
(29) The STO-3G % s values are 46 for the olefinic bond and 38 for the methylene bonds.
(30) (a) C. Edmiston and K. Reudenberg, *Rev. Mod. Phys.*, **35**, 457 (1963); *J. Chem. Phys.*, **43**, S97 (1965); (b) M. D. Newton, E. Switkes, and W. N. Lipscomb, *ibid.*, **53**, 2645 (1970).
(31) D. R. Lide, Jr., *J. Chem. Phys.*, **33**, 1514 (1960).
(32) R. D. Nelson, Jr., D. R. Lide, Jr., and A. A. Margott, *Natl. Stand. Ref. Data Ser., Natl. Bur. Stand.*, **No. 10** (1967).
(33) M. D. Harmony, C. S. Wang, K. B. Wiberg, and K. C. Bishop III, *J. Chem. Phys.*, **33**, 3312 (1975).
(34) L. Radom, W. A. Lathan, W. J. Hehre, and J. A. Pople, *J. Am. Chem. Soc.*, **93**, 5339 (1971).
(35) M. J. Dewar, "Hyperconjugation", Ronald Press, New York, N.Y., 1960.
(36) H. Nakatsuji, *J. Am. Chem. Soc.*, **96**, 24 (1974).
(37) S. Rothenberg, *J. Am. Chem. Soc.*, **93**, 68 (1971).
(38) R. L. Kelly, R. Rollefson, and B. S. Schurin, *J. Chem. Phys.*, **19**, 1595 (1951).
(39) A. R. H. Cole and A. J. Michell, *Spectrochim. Acta*, 739 (1964).
(40) D. E. Williams, *Acta Crystallogr., Sect. A*, **30**, 71 (1974).
(41) A. Warshel and S. Lifson, *J. Chem. Phys.*, **53**, 582 (1970).

Basis Set and Electron Correlation Effects on the Total Electron Density in H_2O, H_2S, and BH

Jozef Bicerano, Dennis S. Marynick, and William N. Lipscomb*

Contribution from the Department of Chemistry, Harvard University, Cambridge, Massachusetts 02138. *Received July 18, 1977*

Abstract: The effects of basis set variation and inclusion of electron correlation in ab initio calculations of molecular electronic structure are studied. The ground states of H_2O, H_2S, and BH at their experimental gas phase geometries are chosen for systematic sets of detailed computations using Slater orbital basis sets and ranging in complexity from minimum basis sets to near Hartree–Fock with configuration interaction. Total electron density maps are obtained for each molecule, at each level of approximation, for all planes of interest, and difference density plots are calculated and discussed.

Introduction

Electron density maps have been used for many years to visualize electron distributions in molecules.[1] They have considerably sharpened the chemist's intuition, since a visual representation of electron density can yield information and draw attention to effects otherwise not fully appreciated by examination of a cumbersome set of numbers, such as a wave function or a density matrix.

The most common types of distribution maps used previously are orbital wave function, orbital and total density, and atomic and ionic difference density plots. The latter are supposed to show the changes in electron distribution as atoms or ions are brought together to form the molecular system. Although these maps have contributed considerably to our understanding of chemical bonding, they have been marred by the arbitrariness of the atomic or ionic states used. This situation arises because atoms in molecules are best viewed as modified to some degree,[2] thus creating an ambiguity as to which type of atomic density is the most relevant. Individual orbital density plots, though also quite helpful, suffer from the fact that the same total electron distribution can be partitioned among orbitals in a multitude of ways, the grounds for a given selection being convenience in the study of some chemical or physical property.

Total electron densities, however, are directly related to experiment, and are free from the aforementioned arbitrariness and ambiguities. Hence, they are more relevant for a broad general study intended to analyze the geographical properties of the electron distribution itself, rather than a particular molecular property which depends on it.

Theoretical electron distributions are known to be highly sensitive to the basis set used to expand the molecular wave functions, and in addition electron correlation makes a second-order contribution to the ground-state one-electron density function of a closed-shell molecule. Consideration of these two types of dependences can aid in understanding and interpreting many features of chemical bonding, as well as the variation of

0002-7863/78/1500-0732$01.00/0 © 1978 American Chemical Society

Table I. Coordinates[a,b]

		x	y	z
H_2O[c]	O	0.0	0.0	0.0
	H	0.0	1.430 47	1.107 19
	H	0.0	−1.430 47	1.107 19
H_2S[d]	S	0.0	0.0	0.0
	H	0.0	1.809	1.740
	H	0.0	−1.809	1.740
BH[e]	B	0.0	0.0	0.0
	H	0.0	0.0	2.336

[a] Atomic units. [b] Experimental geometries. [c] Reference 4. [d] Reference 5. [e] Reference 6.

the numerical values of various molecular properties. Therefore, it is surprising to find a very limited number of studies attempting to demonstrate the basis set and correlation effects on total electron densities for a systematically chosen hierarchy of ab initio computations of gradually increasing complexity. The present study is intended to help bridge this gap.

The molecules examined are H_2O, H_2S, and BH, their choice having been dictated by both computational and chemical considerations. All of these molecules are small enough to enable detailed sequences of ab initio calculations to be carried out. H_2O contains, in the simplest way possible, most of the interesting representative characteristics of more complicated molecules, such as an inner shell, lone, and bonding electron pairs. Comparison with H_2S reveals the effects of going down a period, i.e., increasing the number of full inner shells and decreasing the electronegativity of a constituent atom in an isoelectronic sequence. Finally, the molecule BH is sufficiently small to allow a study of inner shell correlation effects.

For H_2O, the first two basis sets used are fully optimized isotropic (MBS) and anisotropic (AMBS) minimum basis sets. These are followed by a double ζ (DZ) calculation. Next, there is an s,p-saturated (SPSAT) computation using a double ζ inner shell, three s-type and four p-type valence shell orbitals for oxygen, and triple ζ basis (1s1s2s) for hydrogen. The augmentation of this basis set with a set of d functions on oxygen leads to a basis set denoted P1D, and a further extension by using a set of p-type polarization functions on the hydrogens is referred to as the P1DP basis. Finally, a near Hartree-Fock (NHF) calculation is done using an SPSAT basis set augmented by two sets of d orbitals on the oxygen and one set of p orbitals on each of the hydrogens. This is followed by a NHF plus valence single-double CI(VCI) calculation which uses the configuration interaction method to treat electron correlation. In addition, a calculation employing a polarized double ζ (PDZ) basis set is carried out, with the DZ basis set augmented by a single set of d orbitals on oxygen and a set of p functions on each hydrogen. Even though this calculation falls outside the logical sequence described above, it was deemed desirable to study the difference between the PDZ and NHF basis sets, since the PDZ bases (or their Gaussian equivalents) are commonly used in many molecular calculations.

For H_2S, a valence-shell optimized MBS calculation is followed by DZ, and then an SPSAT computation employing double ζ inner shells and triple ζ valence shells. Then, P1D, P1DP, NHF, and NHF + VCI calculations are carried out, each level including the same type of new feature as in the corresponding H_2O case.

Inner shell correlation effects, which are excluded from these calculations owing to considerations of computation time, are then studied using BH, for which a NHF (double ζ inner shell, triple ζ plus polarization valence shells) calculation is followed by NHF + VCI and NHF + CI computations, the latter also including single and double excitations from the inner shell.

It should be noted that the NHF calculations reported here are not actually the most complete possible, as higher order spherical harmonics (f, etc.) are neglected. As a consequence, the best variational energy to date is obtained only for H_2S, but not for H_2O or BH. Nevertheless, the difference in electron density between our NHF calculations and the actual Hartree-Fock limit is expected to be very small.

Computational Details

SCF-CI Calculations. The calculations were performed with computer programs previously described.[3] Slater-type basis sets and gas-phase ground state experimental geometries were used. Tables II-IV give some computational details for H_2O, H_2S, and BH, respectively, including sources for the orbital exponent sets used.

The valence shell CI calculations, which were carried out on all three molecules, included all single and double excitations from the valence shell into unoccupied molecular orbitals with SCF eigenvalues less than 9.0 atomic units. Previous

Table II. Basis Sets and Total Energies for H_2O

Level of approximation	Exponents	Energy, au	$\Delta_{ij} = \lvert E_i - E_j \rvert$
(1) MBS	O 1s(7.663 03), 2s(2.248 25), 2p(2.214 52)	−75.7032	
	H 1s(1.268 47)		Δ_{ab} = 0.0169
(b) AMBS[a]	O 1s(7.663), 2s(2.251), $2p_z$(2.198), $2p_x$(2.115), $2p_y$(2.482)	−75.7201	
	H 1s(1.241)		Δ_{bc} = 0.2850
(c) DZ[b]	O 1s(9.466 35), 1s(6.837 68), 2s(2.688 01), 2s(1.675 43), 2p(3.694 45), 2p(1.658 64)	−76.0051	
	H 1s(1.306), 2s(1.343)		Δ_{cd} = 0.0189
(d) SPSAT	O 1s(12.418), 1s(6.995), 3s(8.681), 2s(2.922), 2s(1.818), 2p(8.450), 2p(3.744), 2p(2.121), 2p(1.318)	−76.0240	
	H 1s(2.459), 1s(1.325), 2s(2.320)[c]		Δ_{de} = 0.0302
(e) P1D	Basis set (d) plus O 3d(2.122)[d]	−76.0542	Δ_{ef} = 0.0086
(f) P1DP	Basis set (e) plus H 2p(1.99)[c]	−76.0628	Δ_{fg} = 0.0011
(g) NHF	Basis set (d) plus O 3d(2.824), 3d(1.636)[e]	−76.0639	
	H 2p(1.99)		Δ_{gh} = 0.2311
(h) NHF + VCI	Same as (g)	−76.2950	
(i) PDZ	Basis set (c) plus O 3d(2.122), H 2p(1.99)	−76.0499	
Best previous variational energy	See ref 10	−76.3683	

[a] The exponents, wave function, and slightly different geometry used are given in ref 7. [b] Oxygen exponents are from ref 8. Hydrogen exponents are from unpublished calculations by R. M. Stevens on diatomic OH with a large basis set. [c] The hydrogen exponents are from ref 9. [d] Unpublished work by R. M. Stevens. [e] Estimates made in the present work.

Table III. Basis Sets and Total Energies for H_2S

Level of approximation	Exponents	Energy, au	$\Delta_{ij} = \lvert E_i - E_j \rvert$
(a) MBS[a]	S 1s(15.5409), 2s(5.314 29), 3s(2.150 58), 2p(5.988 48), 3p(1.868 07)	−397.7921	
	H 1s(1.173 45)		$\Delta_{ab} = 0.8667$
(b) DZ[b]	S 1s(17.0772), 1s(12.6944), 2s(6.728 75), 2s(5.242 84), 3s(2.662 21), 3s(1.687 71), 2p(9.512 51), 2p(5.120 50), 3p(2.337 93), 3p(1.333 31)	−398.6588	
	H 1s(1.367 50), 2s(1.502 42)		$\Delta_{bc} = 0.0042$
(c) SPSAT[c]	S same 1s, 2s, 2p exponents as in (b), but 3s(2.84), 3s(2.18), 3s(1.52), 3p(2.47), 3p(1.81), 3p(1.24)	−398.6630	
	H 1s(2.459), 1s(1.325), 2s(2.32)		$\Delta_{cd} = 0.0408$
(d) PlD	Basis set (c) plus S 3d(2.141 99)[d]	−398.7038	$\Delta_{de} = 0.0096$
(e) PlDP	Basis set (d) plus H 2p(1.99)[f]	−398.7134	$\Delta_{ef} = 0.0003$
(f) NHF	Basis set (c) plus S 3d(2.66), 3d(1.63)[e]	−398.7137	
	H 2p(1.99)		$\Delta_{fg} = 0.1730$
(g) NHF + VCI	Same as (f)	−398.8867	
Best previous variational energy	See ref 11	−398.6862	

[a] Sulfur inner shell exponents are from ref 8. [b] Sulfur double ζ exponents are from ref 8. The hydrogen exponents are estimates giving the best total energy among the sets of possibilities tried. [c] The sulfur valence shell exponents are from unpublished calculations by D. A. Dixon and D. S. Marynick. The hydrogen exponents are identical with those used in the s,p-saturated H_2O calculation. [d] Reference 12. [e] Estimates made in the present work. [f] Reference 9.

Table IV. Basis Set and Total Energies for BH

Level of approximation	Exponents	Energy, au	$\Delta_{ij} = \lvert E_i - E_j \rvert$
(a) NHF[a]	B 1s(7.338), 1s(3.996), 2s(1.724), 2s(1.110), 3s(4.796), 2p(4.558), 2p(1.753), 2p(0.931), 3d(1.490)	−25.1299	
	H 1s(2.459), 1s(1.449), 2s(1.0205), 2p(1.952)		$\Delta_{ab} = 0.0882$
(b) NHF + VCI	Same as (a)	−25.2181	$\Delta_{bc} = 0.0247$
(c) NHF + CI	Same as (a)	−25.2428	
Best previous variational energy	See ref 14	−25.2621	

[a] A basis set described in ref 13 was augmented by H1s(2.459).

Table V. Contour Levels[a]

(a) Total density maps	(b) Difference maps
10.0	0.032
1.5	0.016
0.75	0.008
0.45	0.004
0.28	0.002
0.14	0.001
0.07	−0.001
0.022	−0.002
0.0072	−0.004
0.0029	−0.008
0.000 96[b]	−0.016
	−0.032
	−0.064
	−0.128
	−0.256

[a] In electrons/(atomic unit)^3. [b] This contour level was omitted from the BH total density plot.

calculations on ammonia suggest that exclusion of higher orbitals should have very little effect on the calculated CI energy.[3] A further calculation on BH also included all such excitations involving inner shell electrons. The valence shell H_2O, H_2S, and BH, and the "complete" BH CI calculations, all of which were carried out with the near Hartree–Fock basis sets, involved 4199, 4537, 775, and 1810 determinants, respectively.

Plots. In order to facilitate direct visual comparison, the same two sets of contour levels were used in all of the plots. The values of the total electron density function were calculated on a plane divided into a grid, with the scale chosen such that eight points always corresponded to one atomic unit.

Table V shows the set of contour levels used in all the total density plots, and those used for all the difference maps.

For H_2O and H_2S, computations were carried out both for the "molecular" (yz) and the "lone pair" (xz) planes (see Table I). BH calculations were only performed in a single plane which included the nuclei.

For each molecule, and in each of the planes considered, first the total density map was obtained. In each case only one of these is shown, since the differences are generally too small to be visible to the naked eye. The difference maps were obtained by subtracting the total densities point by point from one another sequentially in each set.

Figures 1–3 show the total density maps, and Figures 4–9 display the differences calculated from them. These plots are discussed in detail in the following section.

Discussion

H_2O and H_2S. For H_2O, the DZ–AMBS (Figures 4b and 5b) and DZ–MBS (Figures 4c and 5c) plots are very similar. Moreover, the differences manifested in either set of maps are much larger than any others along the sequences. This is consistent with the fact that the largest changes in electron density functions and most molecular properties (i.e., total energy, see Tables II and III) are known to occur in going from

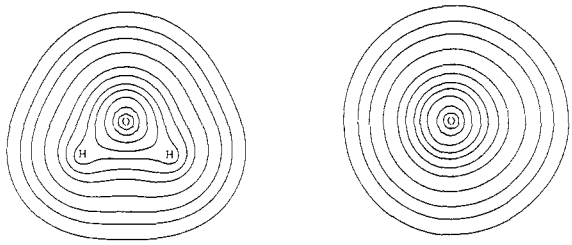

a b

Figure 1. Total electron density maps for H_2O: (a) in the molecular plane; (b) in the "lone pair plane" perpendicular to the molecular plane, and bisecting the H–O–H angle (the z axis increases from left to right). (See Table V(a) for the contour levels.)

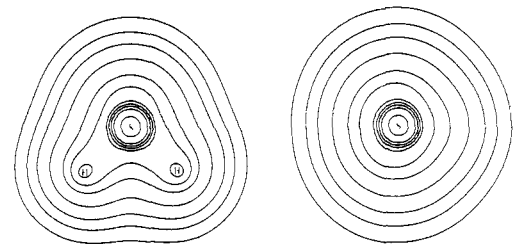

a b

Figure 2. Total electron density maps for H_2S: (a) in the molecular plane; (b) in the "lone pair plane" perpendicular to the molecular plane, and bisecting the H–S–H angle (the z axis increases from left to right). (Same contour levels as in Figure 1.)

a minimum to a DZ basis set. The similarities between the DZ–MBS and the DZ–AMBS plots, as well as the small differences between the MBS and AMBS energies, suggest that using an AMBS is probably not worth the extra computational effort. The deficiencies of an MBS impose restrictions not remedied adequately until the DZ level. Further evidence for the lack of significant improvement upon going from an MBS to an AMBS comes from the AMBS–MBS difference plots (Figures 4a and 5a), which look quite different from the DZ–MBS plots, especially in the molecular plane.

For both H_2O and H_2S (Figures 6a and 7a), there are three major changes which occur upon going from a MBS to a DZ basis. First, the inner regions close to the central atom show a net increase in electron density. Second, in the outer regions on the side of the molecules opposite to the hydrogens, the density also increases. Third, there is a marked decrease in density in the bonding region.

The first two effects are apparently purely of an atomic nature. In fact, DZ–MBS difference plots for the ground states of atomic oxygen and sulfur (not shown) look remarkably similar to these molecular plots in the region opposite the hydrogens.

The decrease of density in the bonding region is accompanied by a very large decrease of density in the area "behind" the hydrogens, i.e., in the region along the H–O axis and opposite the oxygen. This illustrates the fact that the MBS calculation exaggerated the electron density in this region. This excess density, being directed away from the X–H lines, creates forces tending to pull the nuclei apart, thus lengthening the bond. Its partial removal at the DZ level signals a shortening of the bond length, in agreement with well-known trends.[15] On the other hand, there is a net decrease in charge density directly between the hydrogens, in both molecules. This correlates well with the known trend[15] that an MBS tends to underestimate, and a DZ basis tends to exaggerate bond angles.

The H_2O SPSAT–DZ plots (Figures 4d and 5d) reveal a major change in electron density, showing that DZ still leaves much room for improvement, even before the addition of polarization functions to the basis set. Some charge is again removed from behind the hydrogens, and charge accumulates principally along the bond axes. There is a small amount of bond shortening, but the effect on the angle is more ambiguous. Even though there seems to be a net increase of charge between the hydrogens, angle optimizations with these basis sets show that the SPSAT basis tends to give a slightly larger angle than the DZ basis.

The effects displayed in the H_2S SPSAT–DZ plots (Figures 6b and 7b) are much smaller than those for H_2O. Thus, the DZ basis is more successful in describing a third-row atom such as sulfur than a second-row atom like oxygen. Such a result is not unexpected, since the DZ basis for sulfur is made up of six s-type and four p-type functions, all of which can contribute, however slightly, to the description of the valence (and core)

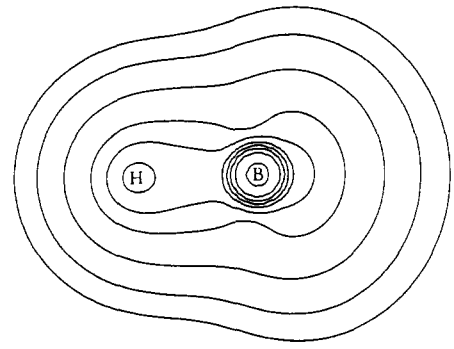

Figure 3. Total electron density map for BH. (See Table V(a) for the contour levels.)

orbitals of the appropriate symmetry. The corresponding basis set for oxygen is clearly not as flexible, especially with regard to p orbitals, which are of course limited to two by definition.

Introduction of d orbitals at the SCF level causes a polarization effect. In the molecular plane, a major increase is seen in the bond regions, encompassing also the entire area between the hydrogens, both for H_2O (Figure 4e) and H_2S (Figure 6c). These effects lead to some bond shortening and a significant angle closing. Later plots show that none of the more elaborate calculations introduces an appreciable effect of this kind in either direction on the bond angle. This is consistent with the common tendency[15] of bond angles in XH_n molecules to approach closely to the NHF (and experimental) values when the first set of heavy atom polarization function is introduced. Electron density is removed from the heavy atom "lone pair" region, and from behind the hydrogens. The "lone pair" plane plots for H_2O (Figure 5e) and H_2S (Figure 4c) also verify the redistribution of electrons from the "lone pair" to the bonding region. This effect is slightly weaker and more complicated for H_2S.

It is very interesting to compare the SPSAT–DZ and SP1D–SPSAT plots for H_2O. Careful examination reveals that, for H_2O, electron redistribution upon proceeding from a DZ to an SPSAT basis is nearly as large as that resulting from the addition of a polarization function to the central atom. This clearly emphasizes the necessity of providing an adequate s,p basis *before* adding polarization functions. We shall return to this point later.

Hydrogen p orbitals strongly polarize the electron distribution around the hydrogens in the bond directions, both for H_2O (Figures 4f and 5f) and for H_2S (Figures 6d and 7d). In addition to this bond shortening effect, the density in the oxygen "lone pair" region increases appreciably in H_2O.

Introduction of a second set of d orbitals in H_2O (Figures 4g and 5g) increases the electron density in the bond regions

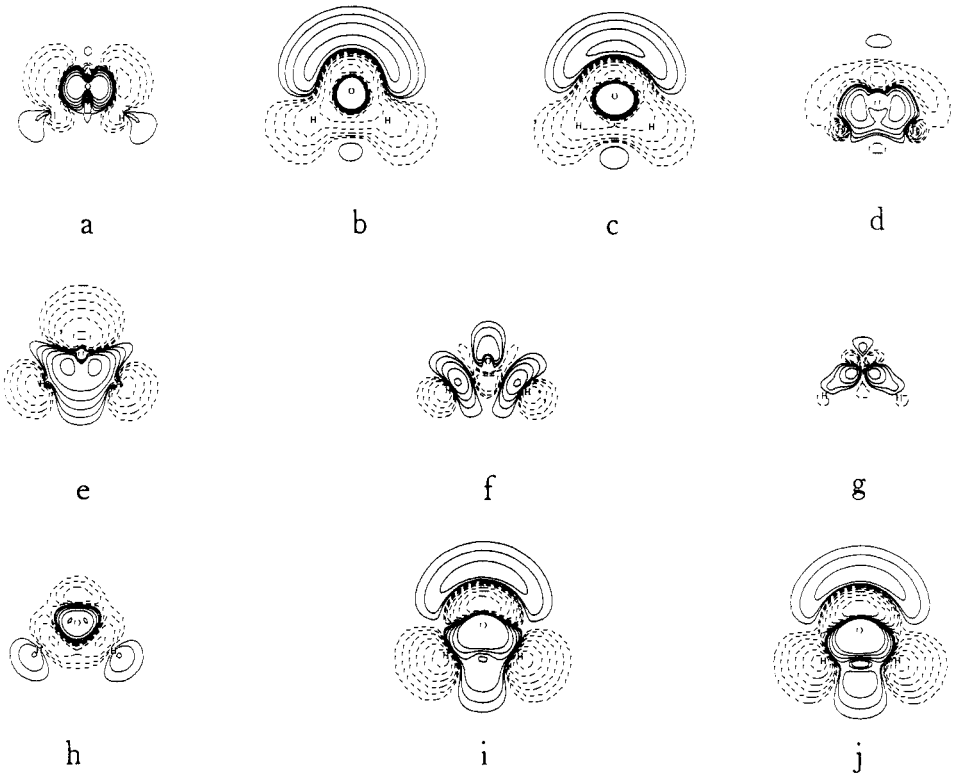

Figure 4. Electron density difference plots for H_2O in the molecular plane. (See Table II for the terminology used.) (a) AMBS-MBS, (b) DZ-AMBS, (c) DZ-MBS, (d) SPSAT-DZ, (e) PID-SPSAT, (f) PIDP-PID, (g) NHF-PIDP, (h) (NHF + VCI)-NHF, (i) NHF-MBS, (j) (NHF + VCI)-MBS. (See Table V(b) for the contour levels.)

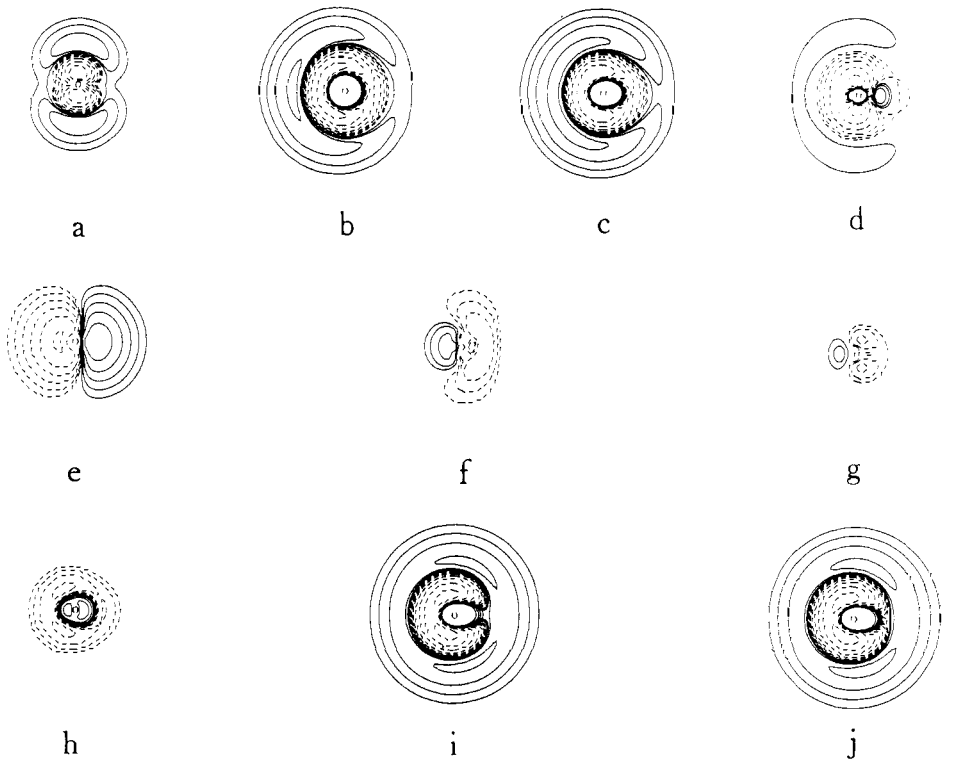

Figure 5. Electron density difference plots for H_2O in the "lone pair plane" perpendicular to the molecular plane and bisecting the H-O-H angle. (The z axis increases from left to right.) (a) AMBS-MBS, (b) DZ-AMBS, (c) DZ-MBS, (d) SPSAT-DZ, (e) PID-SPSAT, (f) PIDP-PID, (g) NHF-PIDP, (h) (NHF + VCI)-NHF, (i) NHF-MBS, (j) (NHF + VCI)-MBS. (Same contour levels as in Figure 4.)

appreciably, as well as removing some more charge from behind the hydrogens. For H_2S (Figures 6e and 7e) the effects of introducing this extra set of d orbitals are far less clear, and much smaller. This sheds an interesting light on the role of d orbitals. The first set had almost the same effect on both molecules, those in H_2O being slightly more pronounced, especially in the "lone pair" plane. The second set still produced clearly understandable changes in H_2O, whereas the effects in H_2S were much smaller. Although the sulfur is not in a state of abnormally high valence (greater than four), it is certainly

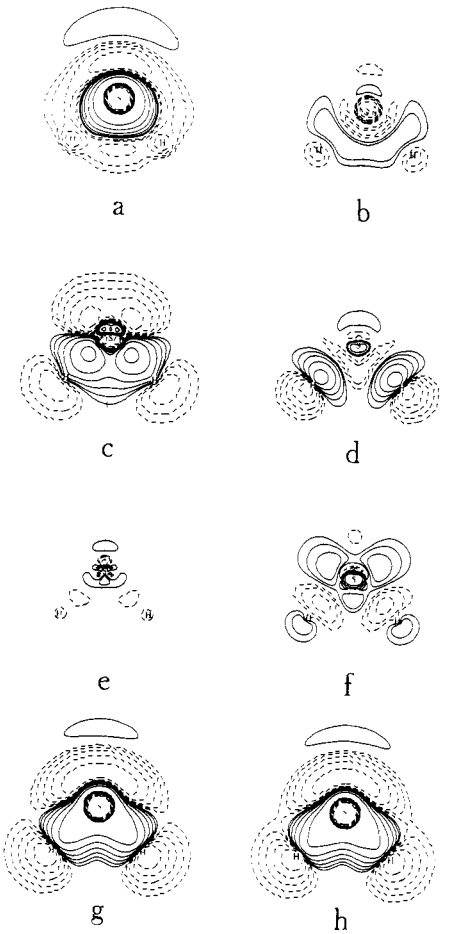

Figure 6. Electron density difference plots for H_2S in the molecular plane. (See Table III for the terminology used.) (a) DZ-MBS, (b) SPSAT-DZ, (c) PID-SPSAT, (d) PIDP-PID, (e) NHF-PIDP, (f) (NHF + VCI)-NHF, (g) NHF-MBS, (h) (NHF + VCI)-MBS. (Same contour levels as in Figure 4.)

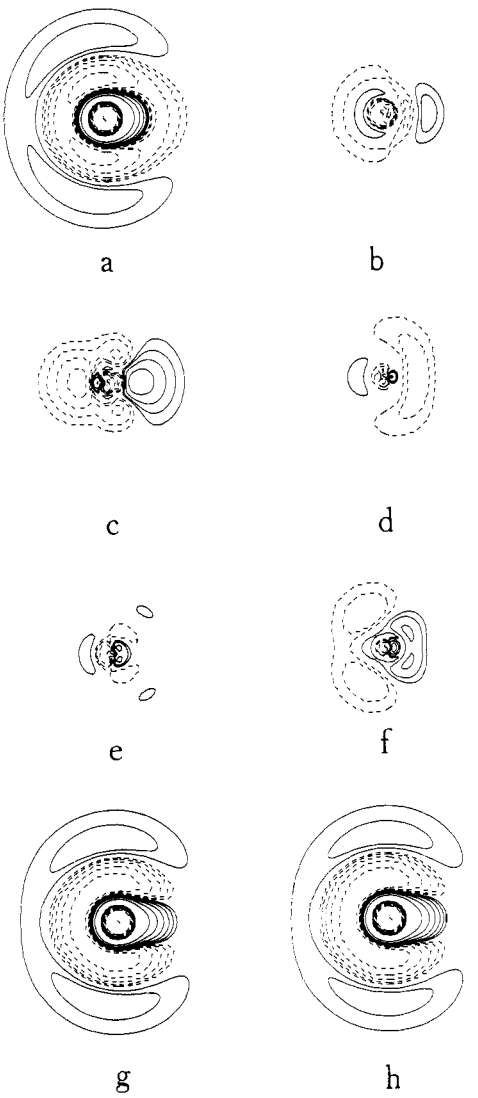

Figure 7. Electron density difference plots for H_2S in the "lone pair plane" perpendicular to the molecular plane and bisecting the H-S-H angle. (The z axis increases from left to right.) (a) DZ-MBS, (b) SPSAT-DZ, (c) PID-SPSAT, (d) PIDP-PID, (e) NHF-PIDP, (f) (NHF + VCI)-NHF, (g) NHF-MBS, (h) (NHF + VCI)-MBS. (Same contour levels as in Figure 4.)

surprising that, using the criterion of degree of electron redistribution, d orbital effects appear to be *as large or even greater* in H_2O as compared to H_2S.

In Figures 4h and 5h, the H_2O (NHF + VCI)-NHF difference densities show charge being transferred from the bond and "lone pair" regions mainly to the area behind the hydrogens. In addition, some extra charge is transferred close to the oxygen nucleus. Figure 4h is similar in all respects to an H_2O (NHF + CI)-NHF difference density plot recently obtained using a Gaussian basis set with the CI including all single and double excitations.[16]

The corresponding plots for H_2S (Figures 6f and 7f) also display charge being removed both from the bond and the "lone pair" regions. This electron density is transferred into the areas behind the hydrogens, into those directly away from the S-H bond axes behind sulfur, and to a lesser extent along the bisector of the bond angle in front of the sulfur. These transfers clearly correspond to charge transfer from all major electron-rich regions into all electron-poor ones. In fact, these effects are clearer for H_2S than for H_2O.

For both molecules, removal of electron density from the bond regions and into the regions behind the hydrogens indicates a bond-lengthening effect. This is in contrast to the basis set variations, where each further augmentation brought a further bond shortening, even if minute.

The major differences between the (NHF + VCI)-NHF plots for H_2O and H_2S are in the regions around the central atom. Plots of the various pseudonatural orbitals (PSNOs) for H_2O and H_2S (not shown) demonstrate that three PSNOs contribute strongly to this region: the $3b_1$ (population 0.0326 e), $6a_1$ (population 0.0268 e), and $1a_2$ (population 0.0164 e). The populations of the corresponding PSNOs in H_2O are 0.0229, 0.0213, and 0.0058, respectively. In the molecular plane the differences between the (NHF + VCI)-NHF maps for H_2O and H_2S are directly related to differences in the b_1 PSNOs mentioned above. The H_2S $3b_1$ PSNO is substantially more diffuse and populated to a greater extent that the corresponding $2b_1$ PSNO of H_2O. In the perpendicular plane, however, the differences are dominated by differences between the $6a_1$ and $4a_1$ PSNOs of H_2S and H_2O, respectively. It is interesting that the a_2 PSNOs, which are dominated by the central atom d orbitals, contribute little to the difference in charge redistribution observed for these two molecules in the planes we have examined.

If the percent redistribution of electron density ρ upon inclusion of VCI is defined as

$$\% = \frac{100|\rho(\text{NHF + VCI}) - \rho(\text{NHF})|}{\rho(\text{NHF + VCI})}$$

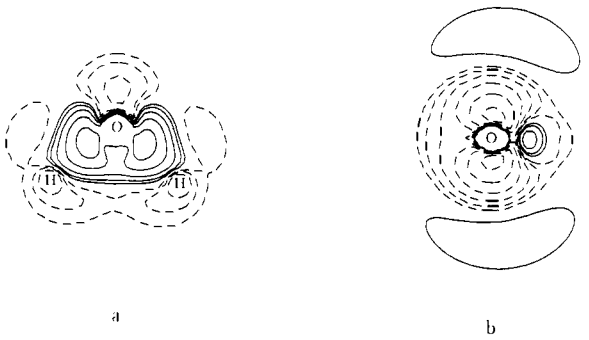

Figure 8. NHF-PDZ density difference plots for H_2O: (a) in the molecular plane; (b) in the "lone pair plane" perpendicular to the molecular plane and bisecting the H-O-H angle (the z axis increases from left to right). (Same contour levels as in Figure 4.)

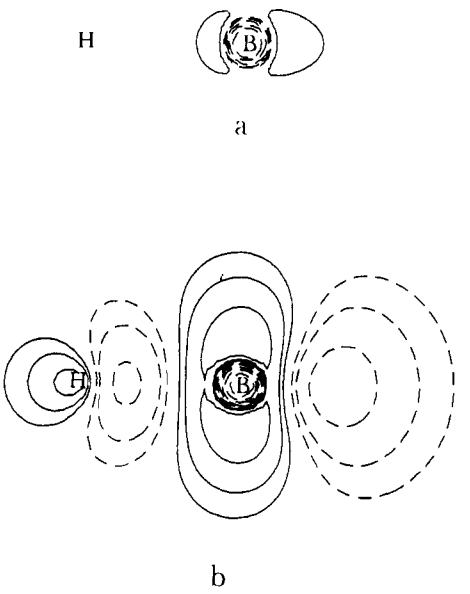

Figure 9. Electron density difference plots for BH. (See Table 4 for the terminology used.) (a) (NHF + CI)-(NHF + VCI). (b) (NHF + CI)-NHF. (Same contour levels as in Figure 4.)

then the maximum percent redistributions for H_2O and H_2S in the valence region are 2.14 and 4.45%, respectively. However, the average values are far smaller.

Both for H_2O and H_2S, in each plane, the NHF-MBS and (NHF + VCI)-MBS plots look nearly identical, illustrating that the effects of introducing electron correlation are much smaller than those of varying the basis set from MBS and NHF. In fact, they are quite similar to the DZ-MBS plots especially in the "lone pair" regions. This is not surprising either, since, as stated before, by far the largest rearrangement of the electron distribution occurs in going from MBS to DZ.

The (NHF + VCI)-MBS plots represent the culmination of all the changes sequentially made. For H_2O (Figures 4j and 5j), they show a net increase of electron density in the bonding region and at the highly electronegative oxygen, and a decrease at the hydrogens. For H_2S (Figures 6h and 7h), much the same effects can be seen. A major difference for H_2S is that in the molecular plane, the excess electron density in the bonding region is quite evently distributed in an almost triangular region defined by the atomic positions.

Figures 8a and 8b display the NHF-PDZ difference plots for H_2O in both planes of interest. These plots are included separately, both because they are outside the logical hierarchy of calculations described above, and because they illustrate what we feel is an important point—that the commonly used PDZ basis set yields densities substantially different from the NHF basis. Comparison of these plots with the SPSAT-DZ plots for H_2O immediately shows that the major deficiency in the PDZ basis is in the lack of s,p saturation—a deficiency which is *not* made up for by adding polarization functions. This situation is not as serious for H_2S, because, as stated before, the DZ basis seems to be substantially closer to the s,p-saturated limit for third-row atoms.

BH. The validity of the interpretation of the results of many studies in electron correlation, including this one, depends on the neglect of inner shell correlation, including this one, depends on the neglect of inner shell correlation effects. Thus, it is desirable to study the consequences of this omission for a small molecle (BH).

Figure 9a demonstrates the (NHF + CI)-(NHF + VCI) difference map for BH, and immediately vindicates the neglect of inner shell correlation, at least in this simple molecule. The differences observed are extremely small. Furthermore, they have essentially no effect in the valence region, as they are immediately around the boron nucleus. Some electron density moves away from the inner shell, most of it going into an area directly along the B-H axis and opposite the hydrogen.

Figure 9b, which shows the (NHF + CI)-NHF plot, is also quite interesting. This plot at first seems anomalous. The expected expansion effect is found at the hydrogen end, where electrons accumulate behind the hydrogen—the usual CI bond lengthening effect, but at the boron end, a considerable density has shifted into the bond region. However, this apparent anomaly is easily resolved: At the SCF level, the three occupied MOs are all of σ symmetry. But there are several low-lying virtual π orbitals with predominant boron $2p_\pi$ character. An examination of the nine most important excitations entering into the CI calculation reveals six of them to be of the type $k\sigma l\sigma \rightarrow m\pi n\pi$, with a final π population of about 0.11 electrons. These excitations are responsible for the increase in density around the boron and perpendicular to the bond axis.

A calculation of the maximum electron density change in the valence region due to inclusion of CI gives 5.86%. As in the cases of H_2O and H_2S, the average percentage redistribution is substantially smaller than this.

Conclusions

The analysis above is mostly qualitative. It could be made more quantitative by, for example, calculating the electron density "flows" into and out of various regions via numerical integration. However, such a detailed analysis is outside the scope of this work, whose main purpose is to contribute to the more intuitive understanding of basis sets and electron correlation effects within the framework of SCF and SCF-CI theories.

Even though the calculations are limited to three molecules, they are sufficiently detailed to show how visual representations of electron densities can aid in understanding many trends in calculated molecular properties. For instance, it is relatively straightforward in most cases to predict bond length and angle trends as a function of basis set and electron correlation by simply examining the difference plots in the molecular plane. Also, it is easy to see from these plots why going from an MBS to a DZ basis produces such large changes in calculated molecular properties, and why, if we can extrapolate our results from BH to other molecules, neglect of inner shell correlation is an excellent approximation for most molecular properties (the most notable exception being the total energy).

In addition, the present calculations draw attention to several points which have often been misunderstood or gone unnoticed. Among these, we may mention: (1) the fact that a DZ basis might be quite different from an SPSAT basis, especially for a second row atom, (2) the demonstration that significant

electron redistribution can occur upon going from a PDZ to a NHF basis, and (3) the fact that, for these molecules, d functions seem to be equally important for a description of the density, even though one of the molecules contains a third row atom.

It should be emphasized that the basis set and electron correlation effects described here are very small compared to the total densities themselves. But the necessity to use adequate basis sets and to include electron correlation to describe many molecular properties correctly is well known. This draws our attention once more to the fact that it is indeed by examining such minute variations of electron distributions that a deeper understanding of chemical bonding is to be reached. Such a circumstance is to be expected, since chemical bonding is a distinctly quantum mechanical phenomenon, arising from a delicate balance of small energy shifts and minute electronic rearrangements.

Acknowledgments. This work was partially funded by the National Science Foundation. The authors thank Dr. R. M. Stevens for the use of his computer programs and for helpful discussions.

References and Notes

(1) See, for example, (a) J. R. VanWazer and I. Absar, "Electron Densities in Molecules and Molecular Orbitals", Academic Press, New York, N.Y., 1975, and references cited therein; (b) P. H. Owens and A. Streitwieser, Jr., "Orbital and Electron Density Diagrams: an Application of Computer Graphics", Macmillan, New York, N.Y., 1973; (c) W. L. Jorgensen and L. Salem, "The Organic Chemist's Book of Orbitals", Academic Press, New York, N.Y., 1973; (d) E. Steiner, "The Determination and Interpretation of Molecular Wave Functions", Cambridge University Press, New York, N.Y., 1976, especially Chapters 6 and 7; (e) E. A. Laws and W. N. Lipscomb, *Isr. J. Chem.*, **10**, 77 (1972); (f) J. D. Petke and J. L. Whitten, *J. Chem. Phys.*, **56**, 830 (1972); **59**, 4855 (1973); (g) A. Støgård, A. Strich, J. Almlöf, and B. Roos, *Chem. Phys.*, **8**, 405 (1975); (h) H. Irngartinger, H.-L. Hase, K.-W. Schulte, and A. Schweig, *Angew. Chem., Int. Ed. Engl.*, **16**, 187 (1977); (i) H.-L. Hase, K.-W. Schulte, and A. Schweig, *ibid.*, **16**, 257 (1977); (j) H.-L. Hase and A. Schweig, *ibid.*, **16**, 258 (1977).
(2) K. Ruedenberg, *Rev. Mod. Phys.*, **34**, 326 (1962).
(3) R. M. Stevens, *J. Chem. Phys.*, **61**, 2086 (1974).
(4) W. S. Benedict, N. Gailar, and E. K. Plyler, *J. Chem. Phys.*, **24**, 1139 (1956).
(5) Recalculated by L. E. Sutton and D. H. Whiffen in "Tables of Interatomic Distances and Configuration in Molecules and Ions", *Chem. Soc., Spec. Publ.*, **No. 18** (1965), using moments of inertia from L. C. Allen and E. K. Plyler, *J. Chem. Phys.*, **25**, 1132 (1956).
(6) S. H. Bauer, G. Herzberg, and J. W. C. Johns, *J. Mol. Spectrosc.*, **13**, 256 (1964).
(7) E. Switkes, R. M. Stevens, and W. N. Lipscomb, *J. Chem. Phys.*, **51**, 5229 (1969).
(8) E. Clementi, and C. Roetti, *At. Data Nucl. Data Tables*, **14**, No. 3-4 (1974).
(9) T. H. Dunning, R. M. Pitzer, and S. Aung, *J. Chem. Phys.*, **57**, 5044 (1972).
(10) W. Meyer, *Int. J. Quantum Chem., Symp. No. 5*, 341 (1971).
(11) S. Rothenberg, R. H. Young, and H. F. Schaefer, III, *J. Am. Chem. Soc.*, **92**, 3243 (1970).
(12) P. E. Cade and W. M. Huo, *J. Chem. Phys.*, **47**, 649 (1967).
(13) E. A. Laws, R. M. Stevens, and W. N. Lipscomb, *J. Am. Chem. Soc.*, **94**, 4461 (1972).
(14) C. F. Bender and E. R. Davidson, *Phys. Rev.*, **183**, 23 (1969).
(15) For an excellent review of methods and results up to 1972, see H. F. Schaefer III, "The Electronic Structure of Atoms and Molecules: A Survey of Rigorous Quantum Mechanical Results", Addison-Wesley, Reading, Mass., 1972.
(16) See Figure 10 in V. H. Smith, Jr., *Phys. Scr.*, **15**, 147 (1977).

Accurate ab Initio Calculations on the Singlet-Triplet Separation in Methylene

Charles W. Bauschlicher, Jr.,*[1a] and Isaiah Shavitt[1a,b]

Contribution from the Battelle Columbus Laboratories, Columbus, Ohio 43201, and the Department of Chemistry, The Ohio State University, Columbus, Ohio 43210.
Received June 13, 1977

Abstract: Configuration interaction (CI) calculations which include all single and double excitations have been performed for the $^3B_1$ and $^1A_1$ states of methylene. The basis sets used were of better than triple-ζ quality and included two sets of polarization functions. The separation is computed to be 10.6 kcal/mol. A trend is shown to exist from the carbon atom through CH to CH_2, which suggests that the actual splitting is less than 10 kcal/mol. This is in disagreement with the interpretation of the latest experimental data, but agrees with earlier experimental work.

I. Introduction

In recent years, there have been a large number of experiments and calculations to determine the singlet-triplet ($^1A_1 - {}^3B_1$) separation for methylene, CH_2. Until recently, there have been two distinct sets of experimental values for this quantity. The high values[2-5] cluster around 7-8 kcal/mol (with the triplet being the ground state), and the lower set[6-8] report 0-3 kcal/mol. The best configuration interaction (CI) results[9] to date have computed the separation to be 14.1 kcal/mol. Other recent calculations[10-13] have also supported the "high" value for the singlet-triplet separation. (An excellent review of earlier work has been given by Harrison.[14])

Very recently, new experimental work by Zittel et al.,[15] based on laser photodetachment spectrometry of CH_2^-, has produced a separation of 19.5 ± 0.7 kcal/mol. Unlike previous experiments, this experiment does not rely on any thermochemical data, but its interpretation depends on the identification and assignment of a peak in the photoelectron spectrum of CH_2^- which is 300 times less intense than the principal peak.

Since the best existing theoretical estimate (14.1) lies between the approximately 8 kcal/mol of the previous "high" value and the 19.5 ± 0.7 kcal/mol of Zittel et al., it is unable to help resolve this difference. For this reason, a new series of high-accuracy ab initio calculations were performed on CH_2.

II. Theoretical Approach

The previous theoretical work (see, e.g., ref 9 and 16) indicates that the triplet state is well described by a single configuration

$$1a_1^2 2a_1^2 1b_2^2 3a_1^1 1b_1^1 \ (^3B_1)$$

The singlet state has been found to have two important con-

0002-7863/78/1500-0739$01.00/0 © 1978 American Chemical Society